Ocean Dynamics (2012) 62:63–76
DOI 10.1007/s10236-011-0487-3

# Inter-annual variability and longer-term changes in the wave climate of Western Australia between 1970 and 2009

**Cyprien Bosserelle · Charitha Pattiaratchi · Ivan Haigh**

Received: 10 May 2011 / Accepted: 3 August 2011 / Published online: 18 August 2011


**Abstract** Quantifying the long-term variability in wave conditions incident on a coastline is critical for predicting its resilience to future changes in the wave climate. In this study, a 40-year wave hindcast of the southern Indian Ocean has been created to assess the inter-annual variability and longer-term changes in the wave climate around Western Australia (WA) between 1970 and 2009. The model was validated against measurements from five wave buoys located along the WA coast. Changes in the mean annual significant wave height, 90th percentile wave height, peak period and mean wave direction were assessed, and the tracks of all wave events generating wave heights above 7 m were digitised and analysed for significant changes. Results show strong annual and inter-annual variability in the mean significant wave height, the 90th percentile wave height and the number of large events (wave height>7 m) that impact the WA coastline. A significant positive trend in annual mean wave height was found in the southwest region of WA over the 40-year simulation. This appears to be due to an increase in intensity of the storm belt in the Southern Ocean which is associated with an increasing positive polarity in the Southern Annular Mode. However, no significant trends were found in the 90th percentile wave height or the number of large wave events impacting Western Australia. Although the number of large wave events in the southern Indian Ocean have increased, their potential to impact the coastal regions of Western Australia are reduced due to storm tracks being located further south, therefore balancing the number of large wave events reaching the WA coast.

**Keywords** Wave climate · Western Australia · Southern Indian Ocean

Responsible Editor: Chari Pattiaratchi

This article is part of the Topical Collection on *Physics of Estuaries and Coastal Seas 2010*

C. Bosserelle (✉) · C. Pattiaratchi · I. Haigh
The School of Environmental Systems Engineering
and the UWA Oceans Institute, University of Western Australia,
35 Stirling Highway, M470,
Crawley, WA 6009, Australia
e-mail: bosserel@sese.uwa.edu.au

## 1 Introduction

Ocean surface waves are the result of momentum and energy exchange between the atmosphere and ocean. Waves carry the energy from storms across ocean basins before being dissipated on the coastline (Snodgrass et al. 1966). Waves transform, refract and break near the shore, generating currents capable of moving sediment over considerable distances. The processes driven by the wave climate also affect the contour of the coast and in particular the shape of sandy beaches.

Wave processes are likely to change in a warming climate (Meehl et al. 2007), and this in turn could alter the rate and direction of sediment transport and ultimately modify the configuration of coastlines (Coelho et al. 2009). Therefore, quantifying potential future changes to the wave climate is an important step to adapt to, and mitigate for, the effects of climate change on the coast. However, it is important to quantify the present and historic wave climate and its variability to provide context for future change as the order of magnitude of the present variability might be greater than the projected change. The aim of this study is to examine the inter-annual variability and longer-term changes in the wave climate around Western Australia (WA) over the past 40 years.

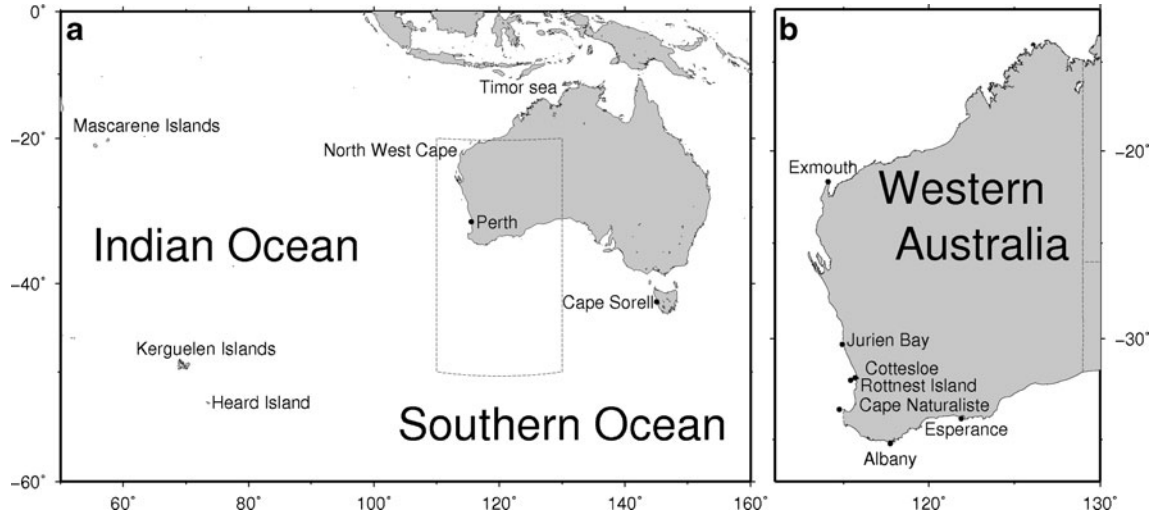


**Fig. 1** **a** The southern Indian Ocean and the area of focus of this study (*dashed line*) and **b** Western Australia and the location of the wave buoys

WA is on the eastern border of the Indian Ocean and northern border of the Southern Ocean (SO). Hereafter, we refer to this area offshore of WA (shown in Fig. 1a) as the southern Indian Ocean (SIO). The SIO is subject to one of the most energetic wave climates in the world (Sterl and Caires 2005). High latitude strong sustained winds (the "Roaring forties") are not slowed by any land mass and can generate large swells which are known to propagate far beyond the SIO (Snodgrass et al. 1966).

Only a few studies have focused on the wave climate of the SIO, in contrast with the North Atlantic which has received considerable scrutiny from the scientific community (Woolf et al. 2002; Wang and Swail 2002; Dodet et al. 2010). The wave climate in the SIO was briefly described by Sterl and Caires (2005) using a global wave climate analysis. They found that the wave climate in SO was less variable than in the North Atlantic but with larger mean wave height, which means the SO is continually rough, whereas the North Atlantic has alternating calm and rough conditions. They also found positive trends in the February mean wave height and in the 99th percentile wave height. More recently, Hemer et al. (2008, 2010) and Hemer (2010) undertook comprehensive studies of the wave climate in the SIO and SO using satellite altimetry, nearshore wave buoy data and model reanalyses. Hemer et al. (2008) found that large wave events around both western and southern Australia are the result of energy propagation from storms running near to the coast rather than the propagation of swell from distant storms. Hemer et al. (2010) found significant positive correlation between wave heights in the SIO and the Southern Annular Mode (SAM), a low-frequency mode of atmospheric variability of the southern hemisphere as well as an anti-clockwise rotation of the wave direction associated with the SAM. They also reported strong positive trends in reanalysis derived wave height (~5 cm/year) in the SIO for the winter months and suggested that this was associated with the positive trend observed in the SAM index. Using reanalysis information, Hemer (2010) found a positive trend in extreme wave heights at Cape Sorell, located in the SO off the Tasmanian coast (Fig. 1a). This finding is interesting given that approximately 20% of the wave events that occur in Cape Sorell are observed beforehand around southwest WA (Hemer et al. 2008). However, this trend was not identified in wave buoy data in the same region. Hemer (2010) warns that the trend could be an artefact from the reanalysis, which is poorly constrained by scarce measurements in the SO. No

**Table 1** Wave Buoys in Western Australia and their duration, location and depth information

| | Longitude (°) | Latitude (°) | Depth (m) | Starting year | Directional year |
|---|---|---|---|---|---|
| Esperance | 121.900 | −34.000 | 52 | 2006 | – |
| Albany | 117.722 | −35.198 | 60 | 2005 | 2008 |
| Cape Naturaliste | 114.764 | −33.535 | 50 | 1999 | 2009 |
| Cottesloe | 115.687 | −31.978 | 17 | 1994 | 2010 |
| Rottnest Island | 115.408 | −32.094 | 48 | 1994 | 2004 |
| Jurien Bay | 114.914 | −30.292 | 42 | 1998 | 2009 |
| Exmouth | 114.099 | −21.699 | 54 | 2006 | 2006 |

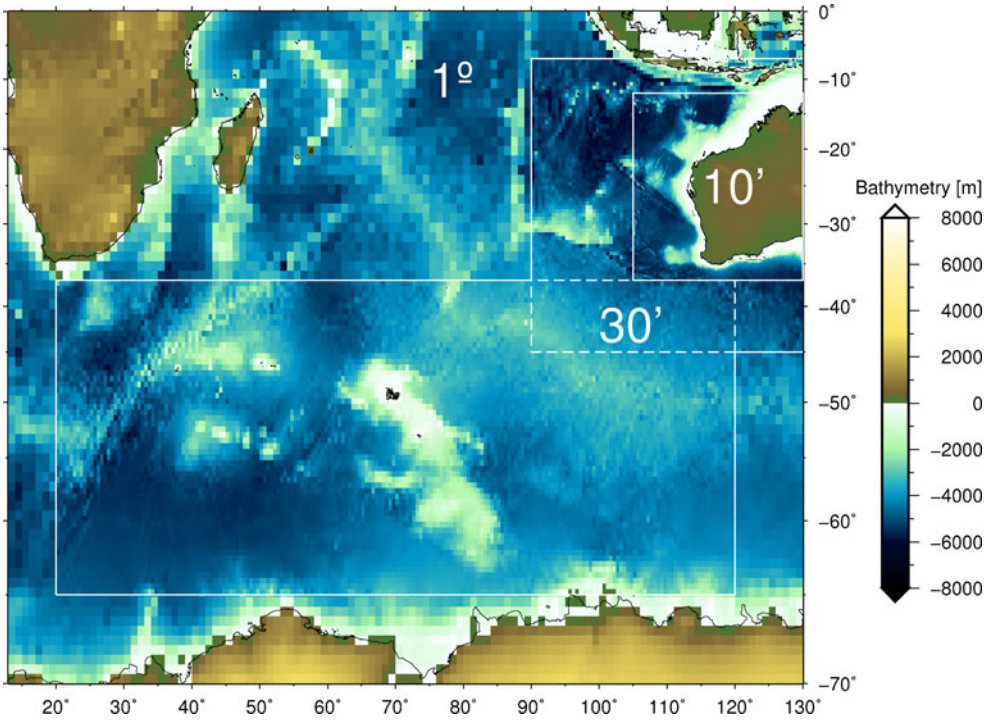


**Fig. 2** Mosaic of bathymetry grids used in WW3; the extent of the figure shows the extent of the coarser grid

satellite altimetry is available in the region prior to 1970, and in situ measurements were generally unavailable prior to the 1990s. This problem was previously identified in the National Center for Environmental Prediction's (NCEP) and National Center for Atmospheric Research's (NCAR) reanalysis wind and sea level atmospheric pressure datasets (Hines et al. 2000; Marshall 2003).

Around WA, systematic wave recordings are rare and relatively short. At Rottnest Island (Fig. 1b) and Cottesloe, continuous wave measurements have been made since 1994. Later, continuous recordings were started at Jurien Bay, then Cape Naturaliste, then Albany and lastly Esperance and Exmouth (Fig. 1 and Table 1). Lemm et al. (1999) described the wave climate at Rottnest Island using 2.5 years of wave buoy record. The fact that the short record analysed included one of the stormiest years for southwest WA (i.e. 1996) most likely biased their results. Further, the record used by Lemm et al. (1999) was too short to adequately evaluate any inter-annual variability. In addition, no directional data were recorded at Rottnest until 2004. Currently there are 16 years of wave data for Rottnest Island, but a minimum of 30 years is recommended by the World Meteorological Organization (IPCC 2007) to undertake detailed analysis of inter-annual variability and to assess longer-term historic trends. The intensification and anticlockwise rotation of the wave climate in the SIO identified by Hemer et al. (2010), neither the intensification nor the rotation of the wave has been identified in Rottnest wave buoy records. This is because of the limited availability of directional wave data in the region.

In this study, due to the limited measured wave record around WA, a 40-year wave hindcast of the SIO has been created and validated against the measured dataset. The wave hindcast record has been used to assess the inter-annual variability and longer-term changes in the wave climate around WA between 1970 and 2009. The work described in this paper is part of a larger study to examine the potential impacts of changes in the wave climate to the sandy coastline of WA. It has been suggested that climate change will drive a southward shift of the storm belt associated with the SAM (Kushner et al. 2001). This could lead to a reduction of the mean wave height around southwest WA, as suggested by Wang and Swail (2006) and Mori et al. (2010), and the rotation of the mean wave direction anti-clockwise (Hemer et al. 2010), which in turn could affect the sediment dynamics in the nearshore. It is therefore important to assess the inter-annual variability of the wave climate around WA and determine if there is

**Table 2** Wave age tuning parameter used for each model grid

| | Grid 1 | Grid 2 | Grid 3 | Grid 4 | Default |
|---|---|---|---|---|---|
| Wave age parameter | 0.015 | 0.016 | 0.016 | 0.018 | 0.011 |

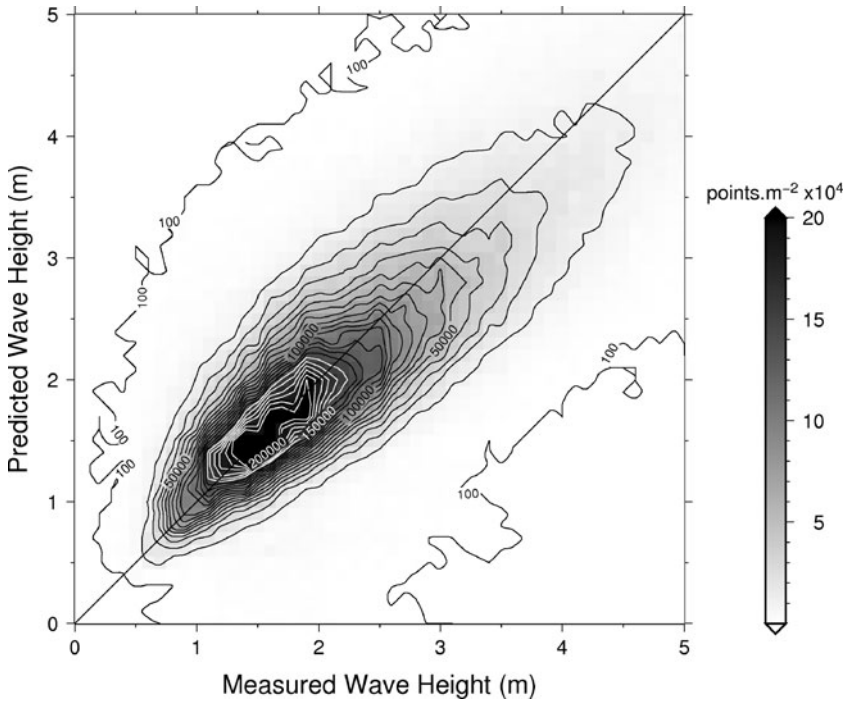


**Fig. 3** Scatter diagram of measured and predicted significant wave height for five wave buoys. The colour scale represents the sample density expressed in number of points per square metre

evidence of any long-term historic changes. This will allow us to better comprehend the consequences potential future changes in the wave climate will have on the WA coast.

The structure of the paper is as follows: Following the introduction in Section 1, a description of the wave model hindcast is presented in Section 2 and the validation exercise is also described. The results are given in Section 3. Section 4 contains a discussion of the key results, and conclusions are given in Section 5.

## 2 Wave model configuration and validation

### 2.1 Model configuration

In order to evaluate the annual and inter-annual variability of the surface ocean waves around WA with high temporal and spatial resolution, a wave model has been set up for the SIO using the WAVE WATCH III ™ version 3.14 (WW3; Tolman 2009). WW3 is used by National Oceanic and Atmospheric Administration for operational global wave prediction. It is a third generation wave model that solves the random phase spectral action density balance equation for wave–number–direction spectra (Tolman 2009).

The model was configured with a domain made up of a mosaic of four grids shown in Fig. 2. These include: a 10-min (~15 km) grid covering the extent of the continental shelf of WA, a 0.5° grid over the southeast Indian Ocean to provide an intermediate resolution to the finer grid, another 0.5° grid covering the storm track in the SO and a 1° grid over the rest of the SIO. The four grids are linked with an obstacle grid to account for islands and shoals that are not resolved by the grid resolution (Tolman 2003). The bathymetric data used to generate all four grids

**Table 3** Statistics of the wave parameters for each wave buoy

| | Albany | Cape Naturaliste | Rottnest Island | Jurien Bay | Exmouth | All |
|---|---|---|---|---|---|---|
| Hs RMSE (m) | 0.70 | 0.59 | 0.50 | 0.54 | 0.32 | 0.53 |
| Hs NRMSE (%) | 29 | 22 | 23 | 25 | 23 | 25 |
| Hs Bias (m) | −0.35 | −0.02 | 0.01 | −0.04 | 0.04 | −0.04 |
| Tp RMSE (s) | 2.9 | 2.7 | 2.7 | 3.0 | 3.4 | 2.8 |
| Tp Bias (s) | −1.5 | −1.4 | −1.1 | −1.2 | −2.1 | −1.3 |
| Mwd RMSE (°) | 21 | – | 24 | – | 50 | 27 |
| Mwd Bias (°) | 3 | – | −17 | – | −32 | −15 |
| Hs RMSEM (m) | 0.41 | 0.16 | 0.14 | 0.36 | 0.09 | 0.26 |
| Hs RMSE90 (m) | 0.81 | 0.07 | 0.19 | 0.52 | 0.13 | 0.41 |

*RMSE* root mean square error, *NRMSE* normalised RMSE, *RMSEM* monthly mean RMSE, *RMSE90* 90th percentile RMSE

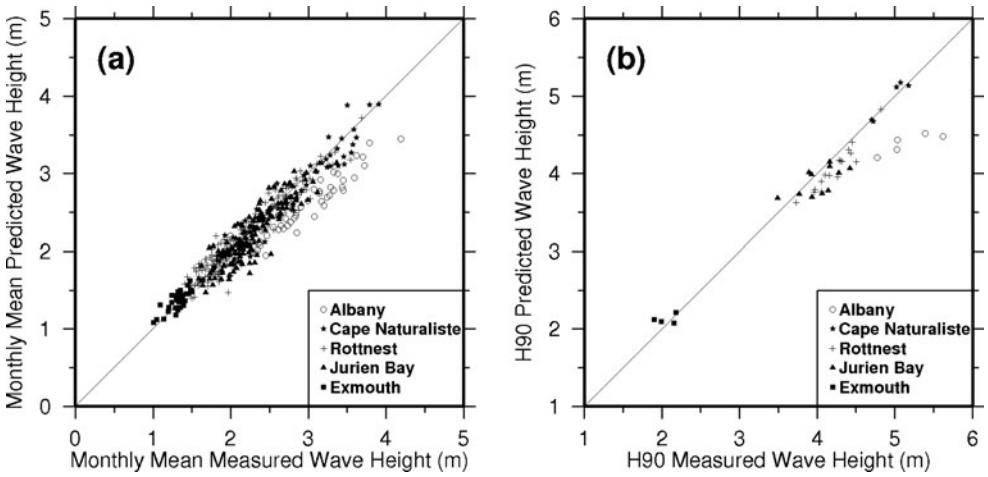


**Fig. 4** **a** Monthly mean wave height validation and **b** yearly 90th percentile wave height validation

were derived from the 2-min global seafloor topography from Smith and Sandwell (1997).

The model was forced with the NCEP/NCAR reanalysis (NNR) wind fields (Kalnay et al. 1996; Kistler et al. 2001). This dataset was selected because its pressure fields are similar than the more recent climate analysis products NCEP/NCAR reanalysis 2 (Kanamitsu et al. 2002) (Pezza et al. 2008). The climate forecast system reanalysis (Saha et al. 2010) is of superior quality, but was unsuitable for this study because of the limited time span (1979 to present). The NNR is a global meteorological reanalysis covering the period from 1948 to present. However, the wave model was only forced with wind fields from 1970 to 2009, representing a 40-year hindcast. The earlier two decades of the NNR were ignored as they are deemed to be unreliable in the SO (Hines et al. 2000). The 6-hourly NNR wind fields

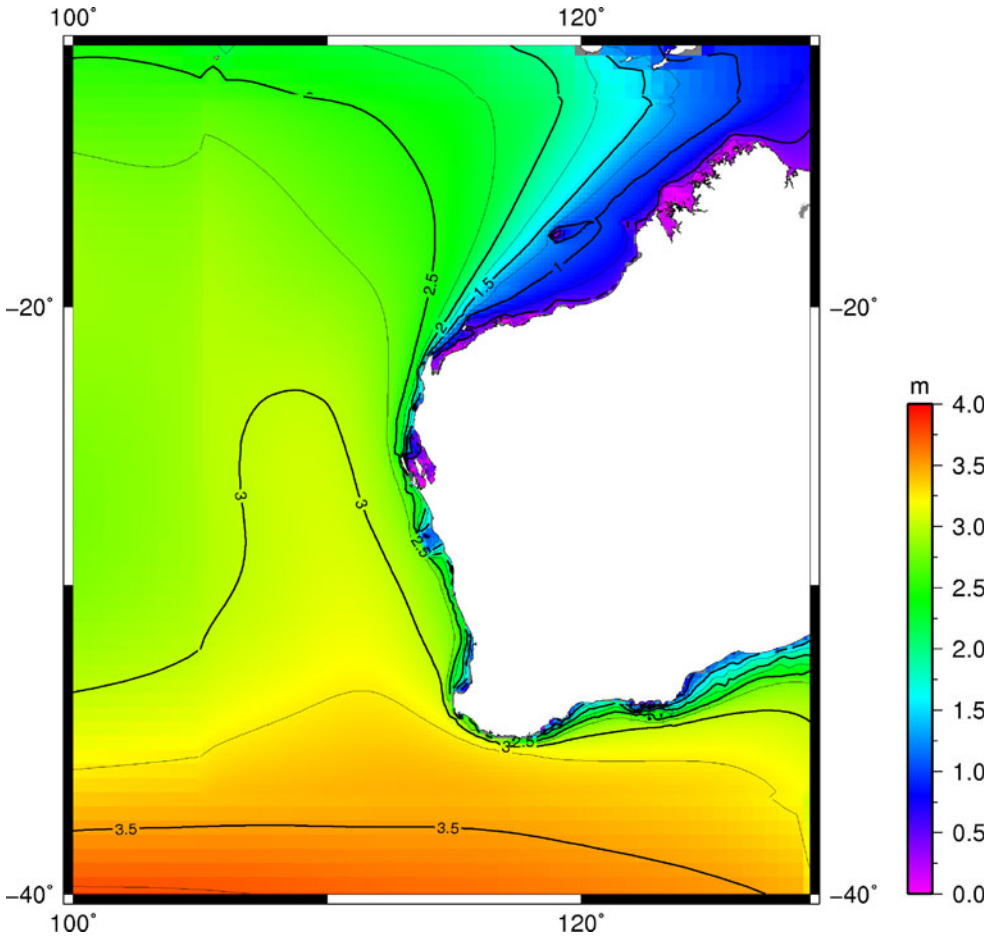


**Fig. 5** Mean significant wave height over the 40-year period (1970–2009) of the model hindcast

are distributed on a gaussian grid and were interpolated to a 1° grid. WW3 automatically interpolates the forcing to the model grids with finer resolution using a quadratic interpolation scheme in both space and time. Although sea ice is present in the SO during the winter months, ice coverage was not included in the model. This is not expected to be a major source of error in the model near WA (Tolman 2003).

The model was parameterised using "WAM 4" definitions and parameters (see Tolman (2009) for details). Only the wave age parameter was adjusted to improve the model accuracy. The values for the wave age parameter for each grid were calibrated; the selected values are presented in Table 2. For more details about the wave age parameter see Ardhuin et al. (2009) .

## 2.2 Model validation

The wave model was validated against measurements from five wave buoys located along the WA coast (Fig. 1b). Details of the duration and location of the wave records are given in Table 1. Esperance was ignored because it is located near to the model boundary. The Cottesloe record was also not used because it is located in shallow water. Each of the five selected wave buoys is located in intermediate water depths (40–60 m; see Table 1).

The 3-hourly model outputs were compared with the measurement data for the periods available at each station. Figure 3 shows the significant wave height scatter diagram of the combined five wave buoy records. The model can be seen to accurately reproduce the significant wave height across the five validation sites with a relatively narrow spread. The root mean square error (RMSE), averaged over the five stations, is 0.53 m with a bias of −0.04 m. RMSE for each station is presented in Table 3. Figure 4a shows the monthly mean measured and predicted wave heights. Again, the model is in very good agreement with the measured data (average RMSE of 0.26 m). This shows that while the model does not capture all the variability of the wave height (i.e. the spread shown in Fig. 3), the mean wave climate is accurately predicted. The model underestimates the mean wave height at Albany (shown by empty circles in Fig. 4a), the continental shelf adjacent to Albany is narrow (approximately 30 km wide) and represented by only two nodes on the finer grid. Hence, the model resolution is likely to be responsible for the

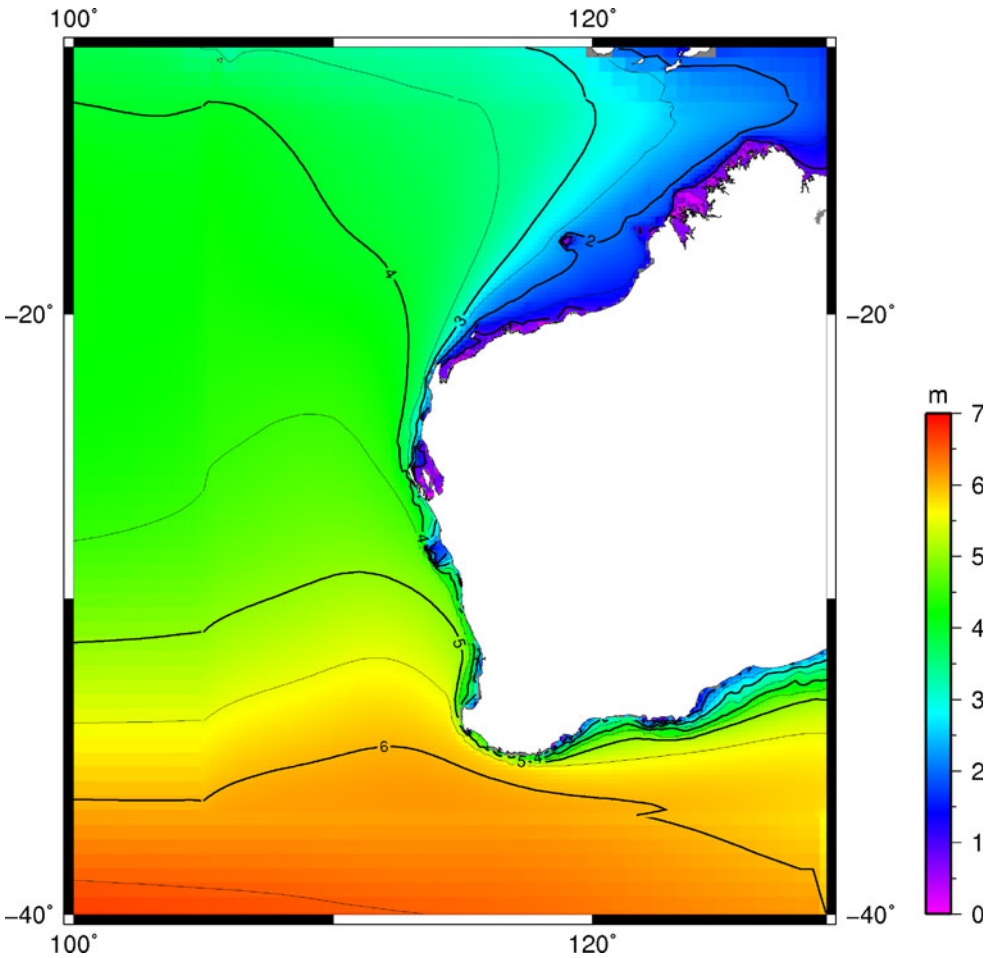


**Fig. 6** Mean 90th percentile wave height over the 40-year period (1970–2009) of the model hindcast

underestimation of the wave height at this location. Figure 4b shows a comparison between the measured and modelled 90th percentile wave height. The results show that the model also accurately predicts the large wave events (average RMSE of 0.41 m), except at Albany where the predicted 90th percentile wave height is underestimated. Peak period and direction RMSE and bias are presented in Table 3.

It has been demonstrated that the model accurately reproduces the wave climate at the five wave buoys located around WA. However, there are categories of wave events that cannot be captured by the model which limits the validity of the model in certain conditions. The wind forcing from NNR is relatively coarse both spatially (1.8°–1.9°) and temporally (6 hourly). As a consequence, some short-lived local winds are under-represented or absent in the wind forcing. This leads to the model not accurately reproducing locally generated short period waves in some regions. This is particularly apparent in summer, when WA is subject to strong shore parallel sea breezes (Masselink and Pattiaratchi 2001). This accounts for most of the model underestimate of the lower range of wave heights shown in Fig. 3. Although the model does not accurately predict these short events, the impact on the mean monthly wave height and annual mean 90th wave height percentile are minimal. On a similar note, because the NNR winds have a frequency of only 6 h, the peaks of storm events tend to be under-represented and this leads to an underestimate of the peak wave height during storms in the model. However, the wave age parameter has been increased in the model to counteract this. Although the simulation of the storm peak was improved for extra-tropical storms, the peak period of the swell was under estimated (up to 2 s; Table 3). The wave age parameter was set to different values for each grid and represents a balance between the best storm peak simulations with the smallest discrepancy in wave peak periods (Table 2).

The other category of wave events that are not likely to be accurately represented in the model are those caused by tropical cyclones crossing the North West Shelf. The spatially and temporally coarse NNR wind fields poorly represent the track and strength of tropical cyclones in the region. In addition, special treatment (Powell et al. 2003) is required (not performed here) to accurately simulate tropical cyclone wave and atmosphere

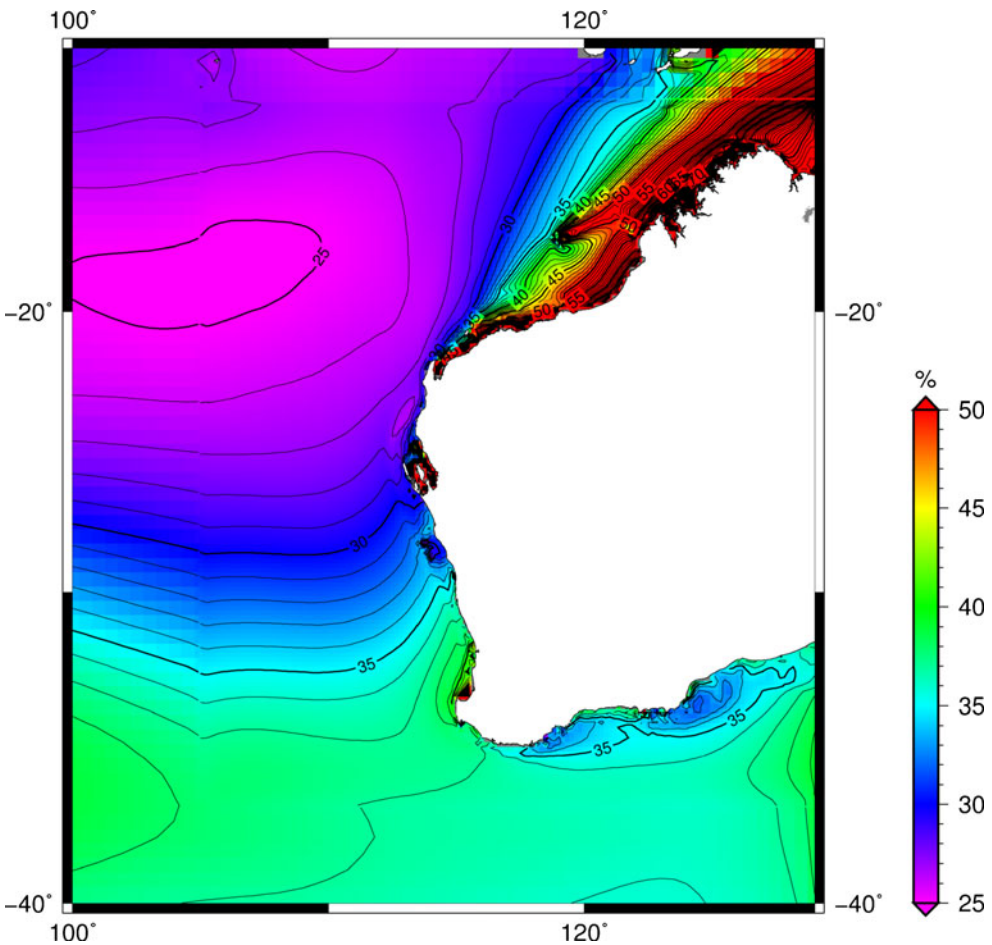


**Fig. 7** Mean annual wave height variability over the 40-year period (1970–2009) of the model hindcast

interaction. These limitations mostly affect the northern coast of WA.

### 2.3 Analysis methods

Several parameters were extracted from the 40-year hindcast to examine the inter-annual and longer-term variability in the wave climate around WA. These were output at 3-hourly intervals and included: the significant wave height, peak wave period and mean wave direction. From these time series mean annual wave heights ($H_S$), peak wave periods ($T_P$) and 90th percentile wave heights ($H_{90}$), which here is defined as the average of the largest 10% significant wave heights, were calculated. The annual mean direction (MWD) was computed by splitting the mean wave direction output into a meridional and zonal component. The two components were averaged and then re-combined. The mean annual variability of significant wave height was calculated by normalising the standard deviation in significant wave height in a given year by the $H_S$ of that year (and hence is dimensionless) and averaging over the 40-year hindcast. The inter-annual variability of $H_S$ was calculated by normalising the standard deviation of the yearly mean $H_S$ by the 40-year mean $H_S$.

Trends in the time-series of $H_S$, $H_{90}$, $T_P$ and MWD were calculated for each node of each model grid. A least square method was applied to find the best linear fit to the 40 annual data points and the $p$ values of the correlation were calculated to identify the significance of the trend. Trends with $p$ values less than 0.05 were considered statistically significant (at 95% confidence).

The tracks of large wave events were digitised to identify the variability of their location. This was done by following local maximum in the grid cells where the significant wave height was larger than 7 m (which equates approximately to $H_{90}$ in the SIO). If more than one maximum was found within a 500-km radius, it was considered as the same wave event and the lower maximum was discarded. If the maximum wave in an event dropped below 7 m for more than 6 h (two output steps), the event was regarded as finished and the track was closed. For each point along a given track, the location of the maximum (latitude and longitude) was recorded as well as the date and time and wave height. Hence, the tracks could be analysed by wave height, location or season. The analysis of

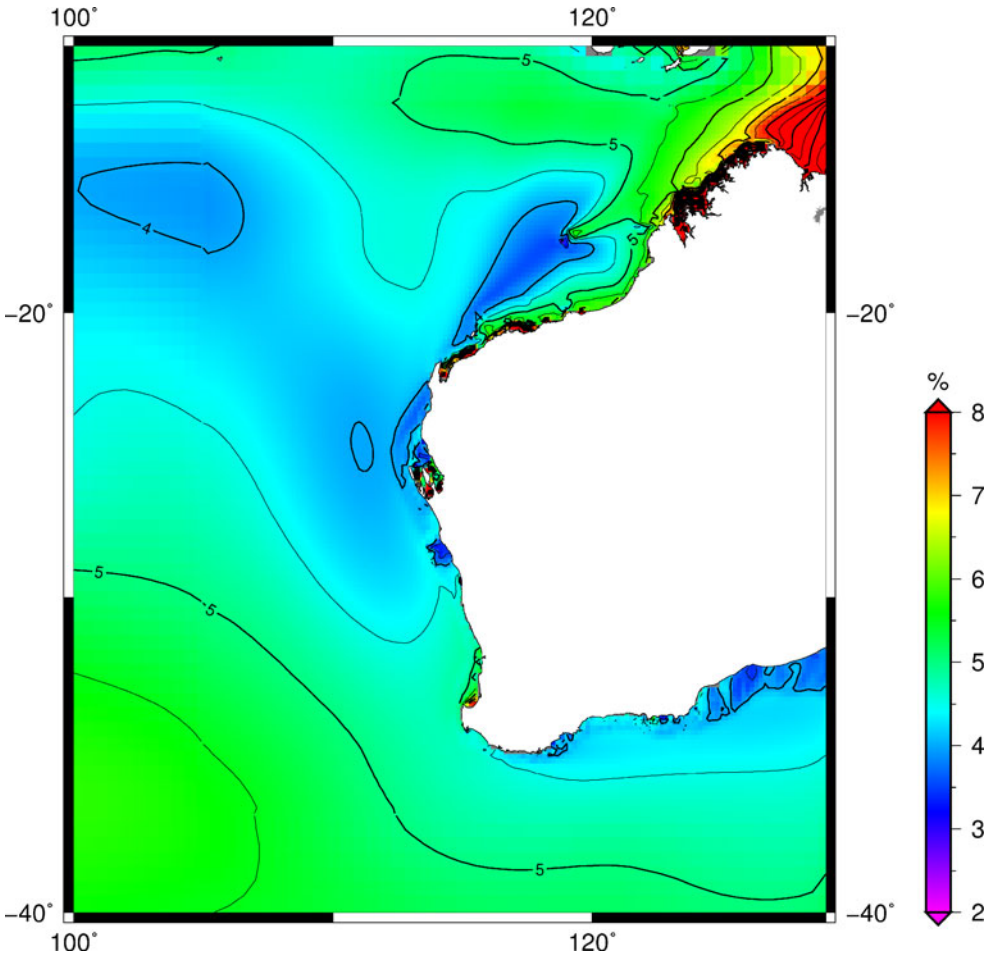


**Fig. 8** Inter-annual wave height variability over the 40-year period (1970–2009) of the model hindcast

wave event tracks was performed for a domain near southwest WA from 110° E to 130° E and between 20° S and 50° S, except for the calculation of the mean latitude of the tracks where all tracks occurring between 110° E and 130° E were taken into account.

The mean annual wave time series and number of large wave events per year have been compared to the SAM index, defined by Marshall (2003). Various definitions of the SAM index have been proposed, but in essence it is a measure of the normalised difference in the zonal mean sea level pressure between 40° S and 65° S. A high positive SAM index equates to a larger pressure difference between 40° S and 65° S. This leads to a strengthening of the circumpolar vortex and an intensification of the westerly winds that encircle Antarctica. The intensification of the high latitude wind band (also called the storm belt) leads to an increase in wave heights in the SO.

## 3 Results

The largest mean $H_S$ (exceeding 4 m) were found in the centre of the storm belt in the SIO. In the SO, between latitudes 30° to 60° S, the strong westerly winds blow uninterrupted, and this region is often referred to as the "roaring forties" and "furious fifties". It is the most energetic region of the global ocean and where the largest mean $H_S$ is found (Sterl and Caires 2005). Closer to WA, the offshore mean $H_S$ is around 3 m (Fig. 5). The northern sector of the state (latitude north of 20° S) has a mean $H_S$ of only 1 m because the region is in the shadow of the North West Cape which blocks most of the waves generated in the SO.

Similar patterns to the mean $H_S$ can be observed in the mean $H_{90}$. In the storm belt, the mean $H_{90}$ height exceeds 7 m, with the exception of the wave shadow created behind the Kerguelen archipelago and Heard Island. The mean $H_{90}$ is larger around the southern part of the WA coast (~5 m) and decrease further north to reach about 3 m around the North West Cape (Fig. 6). The northern sector of the state is in the wave shadow of the continent and only receives a small portion of the wave energy generated in the SIO. However, the $H_{90}$ in this area still exceeds 2 m because of the occasional occurrence of tropical cyclones (although these are not accurately resolved in the NNR wind forcing).

The mean $T_P$ (not shown here) is above 12 s east of the 80° E meridian. Near WA the mean $T_P$ exceeds 13 s. We would expect the $T_P$ to be lower near the coast. The overestimation could be because the strong coastal sea breezes on the WA coastline are not well represented in the wind forcing. In the northern part of WA, in the wave

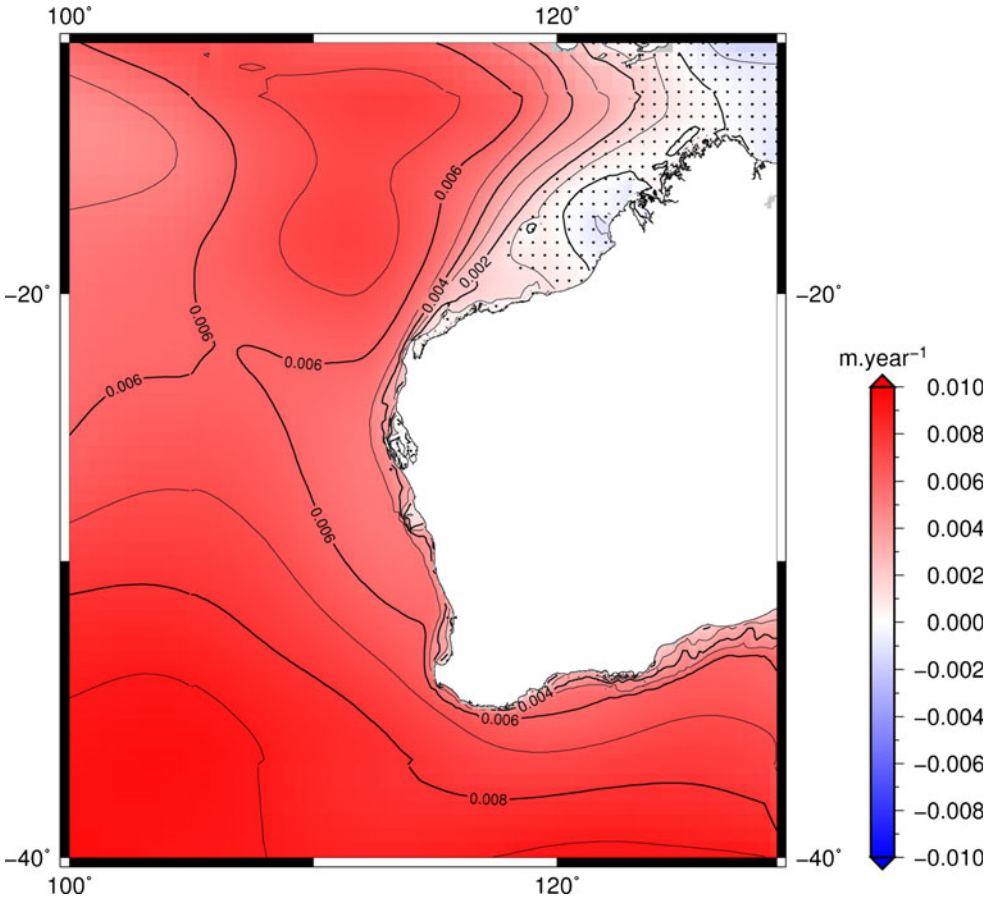


**Fig. 9** Trends in the mean annual wave height over the 40-year period (1970–2009) of the model hindcast (note: *dotted shading* represents non-significant trends at 95% confidence level)

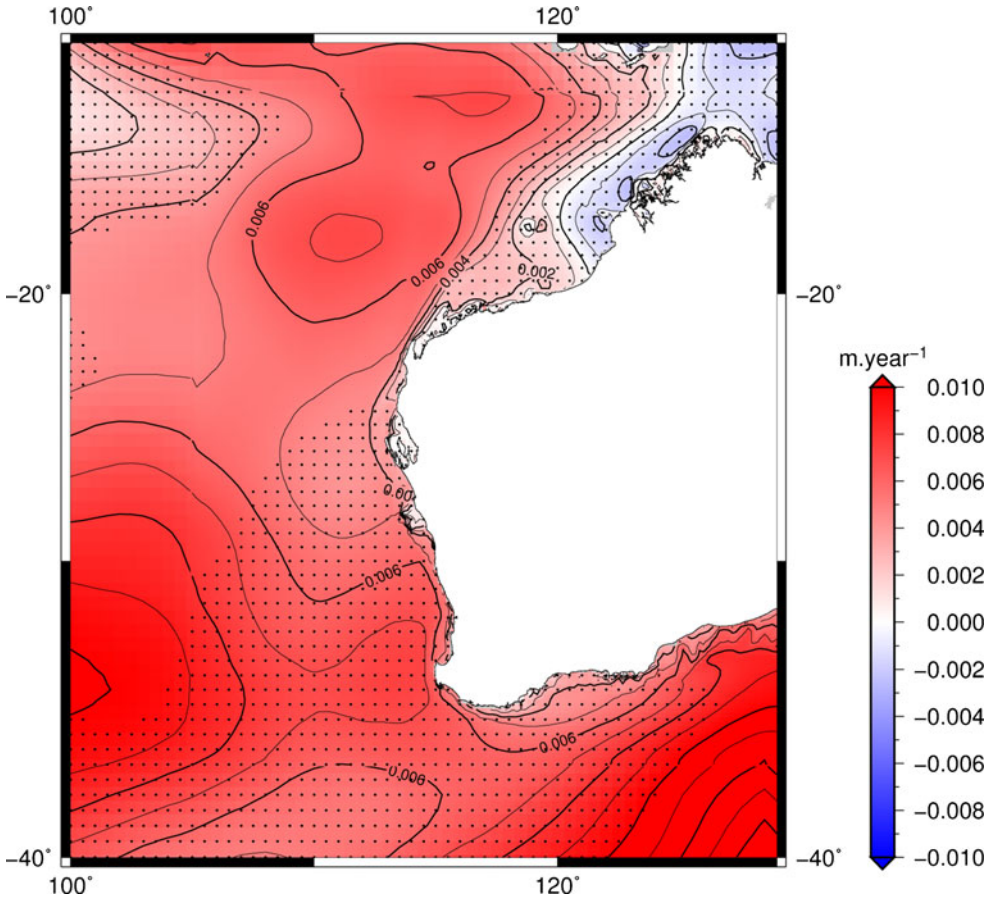


**Fig. 10** Trends in the mean annual 90th percentile wave height over the 40-year period (1970–2009) of the model hindcast (note: *dotted shading* represents non-significant trends at 95% confidence level)

shadow created by the North West Cape where local wind waves dominate, the mean $T_P$ is less 10 s.

The mean MWD (not shown here) is westerly at latitude 50° S, gradually becoming more southerly toward the north and switching to south-easterly near the Mascarenes Islands (Fig. 1). Near WA, the mean MWD is west–south–west along the southern part of the coast and turns gradually south–south–west near the North West Shelf.

The mean annual variability of the significant $H_S$ is shown in Fig. 7. The variability is around 30% across the whole SIO and is largest (>50%) in regions where the mean wave height is lower (i.e. around north WA and nearshore in southwest WA). A region of relatively high variability (>35%) exists across the SIO centred along latitude ~35° S. This area corresponds to the seasonal expansion of the storm belt, when storms track further north in winter.

The inter-annual variability of $H_S$ is ~6% for the whole SIO (Fig. 8). A higher variability (~8%) is present around latitude 60° S (not shown here). Near WA the variability is generally higher in areas where $H_S$ is small (i.e. on the north coast). A region of relatively high variability (>5%) exist offshore of WA (100° E, 40° S).

The 40-year time series of $H_S$, $H_{90}$, $T_P$ and MWD were analysed to identify trends between 1970 and 2009. The time series of $H_S$ shows a positive trend in most of the eastern SIO. The trends are 0.8 cm/year (0.22%/year) in the storm belt which correspond to an increase of 32 cm over the 40 years of this hindcast, and a trend of 0.5 cm/year

**Table 4** Predicted wave climate parameters at the five offshore wave buoy locations

| | $H_S$ (m) | $H_{90}$ (m) | Annual variability (%) | $T_P$ (s) | MWD (°) | Trend $H_S$ (cm/year) | Trend $T_P$ (s/year) |
|---|---|---|---|---|---|---|---|
| Albany | 2.44 | 4.25 | 35 | 13.74 | 214 | 0.42 | 0.019 |
| Cape Naturaliste | 2.63 | 4.86 | 39 | 13.68 | 232 | 0.50 | 0.016 |
| Rottnest Island | 2.14 | 3.98 | 40 | 13.71 | 235 | 0.36 | 0.016 |
| Jurien Bay | 2.18 | 3.87 | 37 | 13.90 | 228 | 0.41 | 0.018 |
| Exmouth | 1.37 | 2.16 | 30 | 13.40 | 228 | 0.25 | 0.014 |

All trends are significant trends at 95% confidence level

(0.2%/year) around WA (Fig. 9) was found. These are statistically significant (95% confidence) and correspond to an 8% (20 cm) increase of $H_S$ near the WA coast over the last 40 years. The $H_{90}$ was also analysed for trends and shows slope of 0.6 cm/year (0.1%/year) in WA corresponding to a 4% increase over the last 40 years. However, no statistically significant trends were found around WA (Fig. 10).

A positive trend in $T_P$ (not shown) was found in the eastern SIO. The strongest trend is observed near Antarctica and WA with an increase of 0.02 s/year. An increase in wave period signifies an increase in swell.

No significant trend in the MWD was found in most of the SIO. There is an anti-clockwise trend in the southern part of the SIO, meaning that waves are becoming more westerly at the high latitudes (i.e. south of latitude 60° S and between 50° E and 110° E) as well as more southerly at the central latitudes (i.e. between 50° S and 30° S and between 50° E and 110° E).

Table 4 summarises the model results at each of the five wave buoy locations around WA. The mean $H_S$ and $H_{90}$ are largest at Cape Naturaliste and then Albany. The annual variability is largest at Rottnest Island and then Cape Naturaliste. These buoys are in the centre of the storm belt winter expansion area and therefore experience the most seasonal change in wave climate with small long period swell in summer and storm waves in winter. At Jurien Bay and Exmouth, located further north, the mean and large wave events heights are smaller. At Jurien Bay, the peak period is larger, as swell travels longer distances to reach this region of the coast.

The tracks of all wave events generating a significant wave height of more than 7 m were digitised for the whole of the SIO. In total, there were ~7,200 events over the 40 years of simulation with an average of 180 per year. Typically, the significant wave height exceeds 10 m for about 23 events per year. The number of large wave events occurring in an area close to WA (between 110° E to 130°E and between 20° S and 50° S as shown in Fig. 1) was calculated for each year for different exceeded wave height values (7, 8, 9, 10 and 11 m) and is presented in Fig. 11. The number of individual events varied considerably from year to year, typically with the minima occurring in the mid 1970s and early 1980s and maxima occurring in 1973, 1996 and 2009. There were no significant trends in the number of events over the 40-year hindcast period for any of the $H_S$ thresholds. This is consistent with the result presented above for the $H_{90}$ around WA.

The 40-year mean latitude at which large wave events cross the 110° E meridian is ~50° S. The annual mean latitudes of the large wave events are presented in Fig. 12 along with the SAM index. There is a large variability in the mean latitude between 1970 and 2009. A correlation (correlation coefficient 0.59) exists between the mean latitude of wave event track and the SAM index. The result shows a significant southward shift in the wave event tracks, corresponding with the trend towards a more positive SAM index.

## 4 Discussion

This study analysed the inter-annual variability and longer-term changes in the wave climate around WA using a 40-year wave hindcast of the SIO. Significant positive trends in $H_S$ between 1970 and 2009 were found around southwest WA. The magnitudes of the trends in $H_S$ were consistent with those found by Young et al. (2011) who analysed altimetry data from 1985 to 2008. However the trends in $H_{90}$ presented by Young et al. (2011) are steeper (0.5%/year) than the finding presented here (0.1%/year). No significant trends were identified in the wave buoy data around WA. The hindcast model is consistent with no significant trend found in the hindcast buoy in the last 15 years. This demonstrated that the use of relatively short period (<30 years) wave records is not sufficient to understand the range in inter-annual variability or longer-term changes in the wave climate.

The agreement between the results presented here and previous work from Hemer et al. (2010) and Young et al. (2011) provided additional validity to the model output, despite the fact that the NNR used here as a forcing to the wave model is known to contain errors in this region. These errors include steeper trends in mean sea level pressure (and by extension to wind) in the SO (Hines et al. 2000). However these steeper trends are only affecting the southernmost part of the SIO (south of 40° S) and are mostly due to a lack of assimilation data in the pre-satellite era (i.e. pre-1970).

The mean latitude at which large wave events propagate near southwest WA (Fig. 12) has been shown to correlate with the SAM Index. A positive SAM index is equivalent to an increased atmospheric pressure gradient between mid and

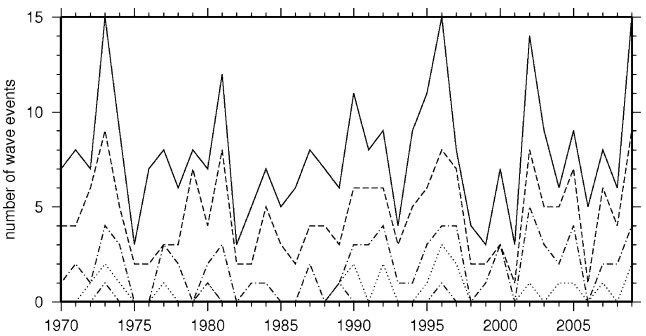


**Fig. 11** Number of wave events over the 40-year period (1970–2009) of the model hindcast calculated in a region offshore of southwest WA for waves exceeding 7 (see Fig. 1; *plain line*), 8 (*dashed line*), 9 (*dot dash line*), 10 (*dotted line*) and 11 m (*dot dot dash line*)

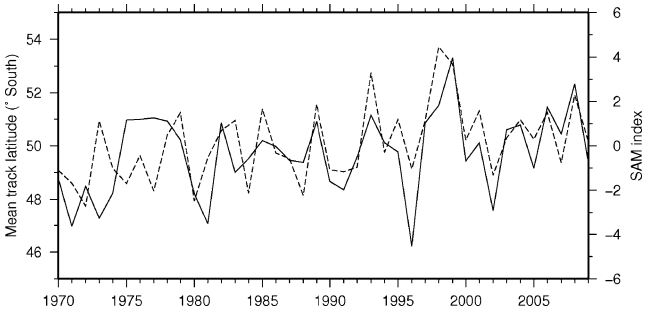


**Fig. 12** Mean latitude at which wave events travel (*plain line*) and SAM index (*dash line*)

high latitudes. These atmospheric conditions tend to prevent storms from tracking northward to the mid latitudes and thus force the predicted wave events to remain at latitudes south of 50° S. Over the last four decades, there has been a significant trend to more positive SAM index (Fogt et al. 2009), which has lead to a southward shift of larger wave events. However, with high variability in the SAM index, years with a low SAM are still relatively common. During years with a low SAM index, the weaker atmospheric gradient tends to allow storms to track at lower latitudes and hence reach the coast of WA, which occurred in 1996 and 2002.

With the southward shift of the storm belt one would expect to see a reduction in the large wave event heights reaching WA. However, no significant trends were found near WA in either the number of larger wave events or in the $H_{90}$. This suggests that while the probability of storm tracking north is reduced, the number of wave events in the SIO has increased over the last 40 years, therefore balancing the number of larger wave events reaching WA. The number of large wave events that reach WA is controlled by a combination of the intensity of the storm belt and the actual pressure gradient between Antarctica and southwest WA, both of which correlated to the SAM index (although the atmospheric pressure is much more variable). During years when the storm belt is highly active, a lot of large storms create large swells; but if the SAM index is high, these events tend to track south of the WA coast (e.g. winter 1999). Inversely, during a calm year in the SO only a few large wave events will be generated; but if the SAM index is negative, these large waves will track north and impact on WA. This is illustrated in Fig. 13, which shows the annual mean track of the larger wave events in 1996 (calm SIO and low SAM) and 1999 (active SIO and high SAM). In 1996, there were three large consecutive storms and the swell they generated significantly eroded the beaches around southwest WA, including the Perth region.

The intensification of the storm belt does not result in an increase of large wave event in WA. However, the intensification of the storm belt also generates more swells.

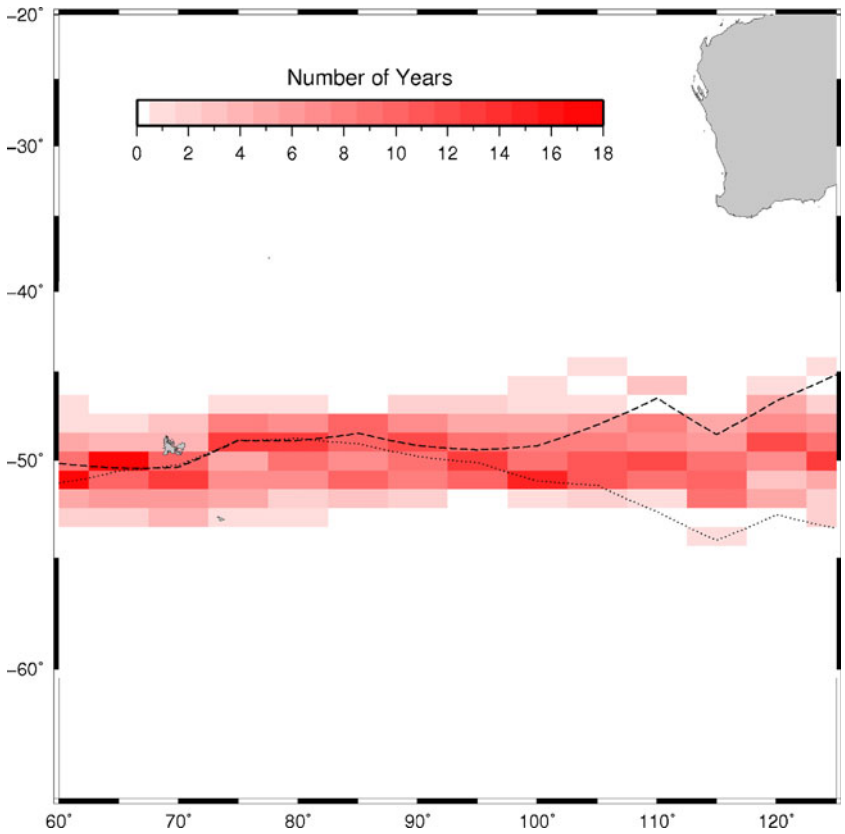


**Fig. 13** Wave event mean track for 1996 (*dashed line*) and 1999 (*dotted line*). The *red shade* shows the range and density of mean tracks over the 40-year period (1970–2009) of the model hindcast

These can travel long distances without being affected by synoptic events. Subsequently these swells propagate to WA coast with enough energy to increasing the average wave height as well as the annual mean $T_P$.

## 5 Conclusions

A wave model has been configured for the SIO to simulate the wave climate around WA during the 40-year period from 1970 to 2009. The model was validated with measured data from five wave buoys located along the coast of WA. The 40-year wave hindcast has then been used to assess the inter-annual and longer-term changes in the wave climate around the WA coastline. The modelled results show that strong annual and inter-annual variability is present in the mean annual significant $H_S$, the $H_{90}$ and the annual mean $T_P$. Results also indicate that there has been a significant increase in $H_S$ and $T_P$ near southwest WA over the past 40 years. It appears that this is a direct consequence of the intensification of the storm belt from where larger swell propagates to WA, thus leading to an increase in $H_S$. However, no significant increases in large wave event heights were found around the WA coastline over the hindcast period. This suggests that although larger wave events are present in the SIO, their probability of reaching Australia is reduced with the trend towards a higher SAM index.

Work is currently underway to evaluate the effect of increasing annual mean $H_S$ and $T_P$ on the morphodynamics of the WA coastline. WA beaches are exposed to a variable wave climate, and their geological and topographical environment is very variable. This diversity means that each beach will respond differently to changes in the wave climate. Moreover, a large fraction (25%) of the beaches in WA are perched, meaning that they are fronted by and/or overlying a shallow rock platform (Stul 2005). Assessing the interaction between an increasing mean sea level, a changing wave climate, the effect of the rock platform and the sediment dynamics is a challenge.

**Acknowledgements** We are grateful to the Western Australian Department of Transport for providing the wave buoy data and for National Oceanic and Atmospheric Administration (NOAA) for providing free access to the WW3 code and the NCEP/NCAR reanalysis. We would also like to thank Tanya Stul for her comments on an early draft of this paper and for many discussions regarding the results. This study was funded through the SIRF scholarship and the Western Australian Marine Science Institution.

## References

Ardhuin F, Marié L, Rascle N, Forget P, Roland A (2009) Observation and estimation of Lagrangian, Stokes, and Eulerian currents induced by wind and waves at the sea surface. J Phys Oceanogr 39(11):2820–2838. doi:10.1175/2009jpo4169.1

Coelho C, Silva R, Veloso-Gomes F, Taveira-Pinto F (2009) Potential effects of climate change on northwest Portuguese coastal zones. ICES J Mar Sci: J du Conseil 66(7):1497–1507. doi:10.1093/icesjms/fsp132

Dodet G, Bertin X, Taborda R (2010) Wave climate variability in the North-East Atlantic Ocean over the last six decades. Ocean Model 31(3–4):120–131. doi:10.1016/j.ocemod.2009.10.010

Fogt RL, Perlwitz J, Monaghan AJ, Bromwich DH, Jones JM, Marshall GJ (2009) Historical SAM variability. Part II: twentieth-century variability and trends from reconstructions, observations, and the IPCC AR4 models, vol 22, vol 20. American Meteorological Society, Boston, MA, ETATS-UNIS

Hemer MA (2010) Historical trends in Southern Ocean storminess: long-term variability of extreme wave heights at Cape Sorell, Tasmania. Geophys Res Lett 37. doi:10.1029/2010gl044595

Hemer MA, Church JA, Hunter JR (2010) Variability and trends in the directional wave climate of the southern hemisphere. Int J Climatol 30(4):475–491. doi:10.1002/joc.1900

Hemer MA, Simmonds I, Keay K (2008) A classification of wave generation characteristics during large wave events on the Southern Australian margin. Cont Shelf Res 28(4–5):634–652. doi:10.1016/j.csr.2007.12.004

Hines KM, Bromwich DH, Marshall GJ (2000) Artificial surface pressure trends in the NCEP-NCAR reanalysis over the Southern Ocean and Antarctica. J Clim 13(22):3940–3952. doi:10.1175/1520-0442(2000)013<3940:ASPTIT>2.0.CO;2

IPCC (2007) Climate Change 2007 - The Physical Science Basis: Working Group I Contribution to the Fourth Assessment Report of the IPCC. Cambridge University Press

Kalnay E, Kanamitsu M, Kistler R, Collins W, Deaven D, Gandin L, Iredell M, Saha S, White G, Woollen J, Zhu Y, Leetmaa A, Reynolds B, Chelliah M, Ebisuzaki W, Higgins W, Janowiak J, Mo KC, Ropelewski C, Wang J, Jenne R, Joseph D (1996) The NCEP/NCAR 40-year reanalysis project. Bull Am Meteorol Soc 77(3):437–472

Kanamitsu M, Ebisuzaki W, Woollen J, Yang S-K, Hnilo JJ, Fiorino M, Potter GL (2002) NCEP-DOE AMIP-II reanalysis (R-2). Bull Am Meteorol Soc 83(11):1631–1643. doi:10.1175/bams-83-11-1631

Kistler R, Collins W, Saha S, White G, Woollen J, Kalnay E, Chelliah M, Ebisuzaki W, Kanamitsu M, Kousky V, van den Dool H, Jenne R, Fiorino M (2001) The NCEP-NCAR 50-year reanalysis: monthly means CD-ROM and documentation. Bull Am Meteorol Soc 82(2):247–267. doi:10.1175/1520-0477(2001)082<0247:TNNYRM>2.3.CO;2

Kushner PJ, Held IM, Delworth TL (2001) Southern hemisphere atmospheric circulation response to global warming. J Clim 14(10):2238–2249. doi:10.1175/1520-0442(2001)014<0001:SHACRT>2.0.CO;2

Lemm AJ, Hegge BJ, Masselink G (1999) Offshore wave climate, Perth (Western Australia), 1994–96. Mar Freshw Res 50(2):95–102. doi:10.1071/MF98081

Marshall GJ (2003) Trends in the southern annular mode from observations and reanalyses. J Clim 16(24):10

Masselink G, Pattiaratchi CB (2001) Characteristics of the sea breeze system in Perth, Western Australia, and its effect on the nearshore wave climate. J Coast Res 17(1):173–187

Meehl GA, Stocker TF, Collins WD, Friedlingstein P, Gaye AT., Gregory JM, Kitoh A, Knutti R, Murphy JM, Noda A, Raper SCB, Watterson IG, Weaver AJ, Zhao Z-C (2007) Global climate projections. In: Solomon S, Qin D, Manning M, Chen Z, Marquis M, Averyt KB, Tignor M, Miller HL (eds) Climate change 2007: The physical science basis. Contribution of working group I to the Fourth Assessment Report of the Intergovernmental Panel on Climate Change. Cambridge University Press, Cambridge, United Kingdom and New York, NY, USA, pp 747–845

Mori N, Yasuda T, Mase H, Tom T, Oku Y (2010) Projection of extreme wave climate change under global warming. Hydrol Res Lett 4:15–19

Pezza AB, Durrant T, Simmonds I, Smith I (2008) Southern hemisphere synoptic behavior in extreme phases of SAM, ENSO, sea ice extent, and Southern Australia rainfall. J Clim 21 (21):5566–5584. doi:10.1175/2008jcli2128.1

Powell MD, Vickery PJ, Reinhold TA (2003) Reduced drag coefficient for high wind speeds in tropical cyclones. Nature 422(6929):279–283

Saha S, Moorthi S, Pan H-L, Wu X, Wang J, Nadiga S, Tripp P, Kistler R, Woollen J, Behringer D, Liu H, Stokes D, Grumbine R, Gayno G, Wang J, Hou Y-T, H-y C, Juang H-MH, Sela J, Iredell M, Treadon R, Kleist D, Delst PV, Keyser D, Derber J, Ek M, Meng J, Wei H, Yang R, Lord S, Hvd D, Kumar A, Wang W, Long C, Chelliah M, Xue Y, Huang B, Schemm J-K, Ebisuzaki W, Lin R, Xie P, Chen M, Zhou S, Higgins W, Zou C-Z, Liu Q, Chen Y, Han Y, Cucurull L, Reynolds RW, Rutledge G, Goldberg M (2010) The NCEP climate forecast system reanalysis. Bull Amer Meteor Soc 91:1015–1057

Smith WHF, Sandwell DT (1997) Global sea floor topography from satellite altimetry and ship depth soundings. Science 277 (5334):1956–1962. doi:10.1126/science.277.5334.1956

Snodgrass FE, Groves GW, Hasselmann KF, Miller GR, Munk WH, Powers WH (1966) Propagation of ocean swell across the pacific. Philos Trans R Soc Lond A, Math Phys Sci 259(1103):431–497. doi:10.1098/rsta.1966.0022

Sterl A, Caires S (2005) Climatology, variability and extrema of ocean waves: the web-based KNMI/ERA-40 wave atlas. Int J Climatol 25(7):963–977. doi:10.1002/joc.1175

Stul T (2005) Physical characteristics of Perth beaches. University of Western Australia, Crawley, Western Australia

Tolman HL (2003) Treatment of unresolved islands and ice in wind wave models. Ocean Model 5:219–231. doi:10.1016/s1463-5003(02)00040-9

Tolman HL (2009) User manual and system documentation of WAVEWATCH III TM version 3.14. NOAA/NWS/NCEP/MMAB Technical Note 276

Wang X, Swail V (2006) Climate change signal and uncertainty in projections of ocean wave heights. Clim Dyn 26(2):109–126. doi:10.1007/s00382-005-0080-x

Wang XL, Swail VR (2002) Trends of atlantic wave extremes as simulated in a 40-yr wave hindcast using kinematically reanalyzed wind fields. J Clim 15(9):1020–1035. doi:10.1175/1520-0442(2002)015<1020:TOAWEA>2.0.CO;2

Woolf DK, Challenor PG, Cotton PD (2002) Variability and predictability of the North Atlantic wave climate. J Geophys Res 107(C10):3145. doi:10.1029/2001jc001124

Young IR, Zieger S, Babanin AV (2011) Global trends in wind speed and wave height. Science. doi:10.1126/science.1197219